Article

J. Biol. Regul. Homeost. Agents. 2024; 38(6): 5271–5283
https://doi.org/10.23812/j.biol.regul.homeost.agents.20243806.421

m^{6}A Demethylase *FTO* Promotes Lung Cancer Progression *in Vitro* and *in Vivo* by Inhibiting *CLIC5*

Ying Xu[1,†], Zhongli Li[1,†], Zhou Cai[1], Lijuan Hu[1], Hong Wu[1,*]

[1]Department of Respiratory and Critical Care Medicine, Zhujiang Hospital of Southern Medical University, 510280 Guangzhou, Guangdong, China
*Correspondence: wuhong_wwho1@163.com (Hong Wu)
[†]These authors contributed equally.

Submitted: 13 March 2024 Revised: 22 April 2024 Accepted: 25 April 2024 Published: 1 June 2024

Background: Lung cancer (LC), a leading cause of cancer-related mortality worldwide, is a major health concern. The N6-methyladenosine (m^{6}A) methylation, a pivotal RNA modification, plays a crucial role in the progression of LC. Therefore, this study aimed to identify m^{6}A modification-related mechanisms underpinning LC progression.

Methods: Expression levels of chloride intracellular ion channel 5 (*CLIC5*), fat mass and obesity-associated protein (*FTO*), and the proto-oncogene tyrosine-protein kinase SRC (SRC) in LC cells and xenograft tumors were assessed utilizing bioinformatics tools, quantitative reverse transcription polymerase chain reaction (qRT-PCR), and Western blot analysis. Furthermore, their interactions were predicted and validated using bioinformatics tools and/or Methylated RNA immunoprecipitation (MeRIP) assay. After *CLIC5*/*FTO* overexpression in LC cells, their roles in LC cell proliferation, migration, invasion, and tumorigenesis were examined employing cell counting kit-8 (CCK-8), 5-Ethynyl-2′-deoxyuridine (EdU), Transwell, and murine xenograft assays.

Results: *CLIC5* was downregulated in LC cells ($p < 0.001$). *CLIC5* overexpression inhibited cell viability, proliferation, migration, invasion, and tumorigenesis in LC ($p < 0.01$). The m^{6}A level was decreased while the *FTO* level was increased in LC cells ($p < 0.001$). *FTO* could interact with the m^{6}A modification site on *CLIC5*, and the m^{6}A methylation of *CLIC5* was potentiated following *FTO* knockdown in LC cells ($p < 0.001$). Furthermore, *FTO* overexpression reversed the inhibitory effect of *CLIC5* overexpression on the proliferation, migration, invasion, and tumorigenesis in LC ($p < 0.05$). Additionally, elevated SRC expression in LC could interact with *CLIC5* ($p < 0.001$). *CLIC5* overexpression diminished SRC expression, and the effect of *CLIC5* on the SRC expression was reversed by *FTO* overexpression.

Conclusions: The downregulation of *CLIC5*, induced by *FTO*-mediated m^{6}A demethylation, facilitates LC progression both *in vitro* and *in vivo*.

Keywords: chloride intracellular ion channel 5; fat mass and obesity-associated protein; Lung cancer; m^{6}A demethylation; cancer progression

Introduction

Lung cancer (LC) has surpassed breast cancer as the leading cause of cancer-related death in women in developed countries and in men around the world [1]. LC is a highly aggressive malignancy with a 5-year survival rate of only 20% [2]. It has been estimated that the global number of LC-related deaths will reach 3 million by 2035 [3], portending a considerable health burden. Unfortunately, despite being a research hotspot for decades, the pathogenesis of LC remains inadequately understood, posing a significant challenge to the development of effective treatment strategies.

Over the past decade, in-depth analyses conducted on LC genomes and signaling pathways have identified LC as a distinct disease characterized by histological, cellular, and molecular heterogeneity [4]. RNA modification has gained much attention in recent years. N6-methyladenosine (m^{6}A) methylation, an essential mRNA modification involved in multiple cellular processes in cancer [5], is the most abundant post-transcriptional mRNA modification. This modification affects mRNA alternative splicing, localization, and stability, thus modulating cancer progression-related protein expressions [6]. The m^{6}A methylation is a dynamic process mediated by m^{6}A methylation controllers, including methyltransferases, binding proteins, and demethylases [7]. Fat mass and obesity-associated protein (*FTO*), a demethylase belonging to the AlkB family, regulates food metabolism and energy expenditure [8]. *FTO* mediates the demethylation of the abundant m^{6}A residues in RNA by regulating oxidative activity [8]. Existing research has uncovered significantly increased *FTO* levels and decreased overall m^{6}A levels in LC tissues [6], suggesting that the reduced m^{6}A levels observed in LC tissues are ascribed to demethylation mediated by the increased *FTO* level. *FTO* is predominantly expressed in multiple cancers and mediates m^{6}A demethylation, stimulating cancer cell metabolism and inducing tumorigenesis and chemoresistance [9,10].

Journal of
BIOLOGICAL REGULATORS
and Homeostatic Agents

Furthermore, *FTO* has been identified as an oncogene in LC [11]; however, the regulatory mechanism of *FTO* in LC remains to be investigated.

This study employed GEO2R to decipher the GSE176348 dataset and predict m^6A-modulated genes exhibiting differential expressions in LC. As a result, chloride intracellular ion channel 5 (*CLIC5*), Transmembrane protein 100 (*TMEM100*), and Surfactant protein A2 (*SFTPA2*) were identified as the top three downregulated genes. *CLIC5,* a member of the CLIC family, forms redox- and pH-sensitive ion channels in planar bilayers and influences cell membrane potential, transepithelial transportation, intracellular pH, and cell volume [12,13]. *CLIC5* has been recognized as the initial mitochondrial chloride channel protein identified within the inner mitochondrial membrane at the molecular level [14]. Previous research has indicated *CLIC5* as a highly expressed oncogenic molecule in acute lymphoblastic leukemia (ALL) [15], hepatocellular carcinoma (HCC) [16], and pancreatic ductal adenocarcinoma (PDAC) [17]. In contrast, reduced expression of *CLIC5* has been identified in osteosarcoma [18]. However, there is no available research regarding the expression pattern and role of *CLIC5* in LC.

Furthermore, functional studies have explored *TMEM100* [19] and *SFTPA2* [20] in LC. Additionally, RMBase v2.0 (https://ngdc.cncb.ac.cn/databasecommons/database/id/4931)-based prediction showed that CLIC has eight m^6A modification sites, one of which binds to *FTO.* Therefore, this study aims to unveil the role of *CLIC5* and its association with *FTO* in the progression of LC.

Objects and Methods

Cell Culture

Human LC cell lines (NCI-H23, NCI-H1650, HCC827 and A549) were obtained from Procell (CL-0397, CL-0166, CL-0094 and CL-0016, Wuhan, China), and human Bronchial Epithelial 16HBE cells were procured from Merck Millipore (SCC150, Billerica, MA, USA). The cells were cultured in Roswell Park Memorial Institute (RPMI)-1640 medium (PM150110, Procell, Wuhan, China) supplemented with 10% fetal bovine serum (FBS; 12103C, Sigma-Aldrich, St. Louis, MO, USA), 1× Glutamax (35050061, ThermoFisher, Waltham, MA, USA), and 1% penicillin-streptomycin (TMS-AB2, Sigma-Aldrich, St. Louis, MO, USA), followed by incubation at 37 °C in a humidified chamber with 5% CO_2. The cells received STR authentication and were free of mycoplasma contamination.

Bioinformatics Analyses

The RMBase v2.0 platform was utilized to predict potential sites for m^6A modification in *CLIC5* and analyze the binding interaction between *FTO* and these sites. The protein-protein interaction (PPI) between *CLIC5* and proto-oncogene tyrosine-protein kinase SRC (SRC) was visualized through STRING (https://www.string-db.org/). Furthermore, StarBase (https://starbase.sysu.edu.cn) was utilized to predict the expression pattern of SRC in LC.

Cell Transfection

Sequences of *CLIC5* (NM_001114086) and *FTO* (NM_001080432.2) were amplified and inserted into pcDNA3.1 vectors (V79520, ThermoFisher, Waltham, MA, USA) to produce overexpression plasmids. pcDNA3.1 empty vector was used as a negative control (NC). Short hairpin RNA targeting *FTO* (sh*FTO*#1, 5′-GCAGCTGAAATATCCTAAACT-3′, siG000079068A-1-5; sh*FTO*#2, 5′-GCTGAAATAGCCGCTGCTTGT-3′, siG000079068B-1-5) and a negative control (shNC, 5′-GGAATCTCATTCGATGCATAC-3′, siN0000001-1-5) were obtained from RIBOBIO (Guangzhou, China). HCC827 and NCI-H1650 cells were transfected with *CLIC5* overexpression plasmids or NC alone, or in combination with *FTO* overexpression plasmids, or with sh*FTO*#1/#2/shNC alone using Lipofectamine 3000 transfection reagent (L3000015, ThermoFisher, Waltham, MA, USA) following the manufacturer's protocols. Briefly, cells were seeded into 96-well plates at a density of 1 × 10^4 cells/well and cultured to 80% confluence. The plasmids and Lipofectamine 3000 transfection reagent, which had been diluted with Opti-MEM media and P3000 reagent, were incubated at 37 °C for 10 minutes to acquire gene-lipid complexes. The cells underwent incubation with the complexes at 37 °C for 48 hours for transfection.

Cell Counting Kit-8 (CCK-8) Assay

After transfection with *CLIC5* overexpression or NC plasmids, HCC827 and NCI-H1650 cells were seeded into 96-well plates (5 × 10^3 cells/well). Subsequently, at 24 and 48 hours of incubation, CCK-8 reagent (C0037, Beyotime, Shanghai, China) was added in one-tenth of the cell culture volume, followed by a 2-hour incubation at 37 °C. Finally, the optical density at 450 nm was assessed using a microplate reader (GM2010, Promega, Madison, WI, USA).

m^6A Content Determination

The overall m^6A levels in NCI-H23, NCI-H1650, HCC827, A549, and 16HBE cells were determined using an RNA Methylation Assay Quantification Kit (ab185912, Abcam, Cambridge, UK) following the manufacturer's instructions. Initially, total RNA was isolated from these cells using Trizol reagent (15596026, ThermoFisher, Waltham, MA, USA). The RNA was then added to the assay well, which contained a binding solution, and the samples underwent incubation with capture antibody at room temperature for 1 hour. After this, the samples were incubated with detection antibody combined with enhancer solution at room temperature for 30 minutes. Color development was performed utilizing a developer solution, and the reaction was

terminated using a stop solution. Finally, the absorbance at 450 nm was assessed within 10 minutes using a microplate reader.

Methylated RNA Immunoprecipitation (MeRIP) Assay

A Magna MeRIP m^6A Kit (17-10499, Merck Millipore, Billerica, MA, USA) was employed to investigate the binding of *FTO* to m^6A modification in *CLIC5*. Briefly, total RNA was extracted from sh*FTO*/shNC-transfected HCC827 and NCI-H1650 cells utilizing Trizol reagent (15596026, ThermoFisher, Waltham, MA, USA). Magnetic beads were then conjugated with m^6A or IgG antibodies through a 1-h incubation, followed by incubation of the antibody-conjugated beads with total RNA for 2 hours at 4 °C. After this, m^6A-containing RNA was immunoprecipitated, treated with proteinase K buffer at 55 °C for 30 minutes, and resuspended with an RNase inhibitor. Finally, the RNA was quantified employing quantitative reverse transcription polymerase chain reaction (qRT-PCR) with *CLIC5* primer (forward 5′-TTTTTTAAGTGGGTAAGGTTGGTAGT-3′, reverse 5′-CACCAAAACCAAAAAAATATCCTAA-3′).

5-Ethynyl-2′-Deoxyuridine (EdU) Assay

After transfection, HCC827 and NCI-H1650 cells were seeded into 96-well plates (4×10^3/well) and subjected to EdU assay using a BeyoClick EdU-594 assay kit (C0078L, Beyotime, Shanghai, China). The cells were cultured with pre-heated EdU working solution at room temperature for 2 hours, fixed with 4% paraformaldehyde (P0018, TCIchemicals, Shanghai, China) for 30 minutes at room temperature, and washed twice with 0.1 mL 3% bovine serum albumin (A1933, Sigma-Aldrich, St. Louis, MO, USA). Subsequently, the cells were reacted with 0.1 mL 0.5% Triton X-100 for 20 minutes. The cells were then exposed to Click-iT EdU reaction solution for 30 minutes at room temperature in the dark. After this, cell nuclei were stained with 4′,6-diamidino-2-phenylindole (DAPI; C1002, Beyotime, Shanghai, China). Finally, fluorescence emitted from proliferative cells was observed using confocal microscopy (LEXT OLS5100, Olympus, Tokyo, Japan) at ×200 magnification.

Transwell Assay

Migration and invasion assays were performed using Transwell chambers with 0.8 μm pore size (3428, Corning Inc., Corning, NY, USA). After transfection with *CLIC5* overexpression plasmids/NC or with *CLIC5* overexpression plasmids and *FTO* overexpression plasmids, HCC827 and NCI-H1650 cells (1×10^5) were resuspended in serum-free RPMI-1640 medium (100 μL), and directly added to the upper chamber for the migration assay. For the invasion assay, the upper chamber was precoated with 50 μL of 1 mg/mL Matrigel (356234, Corning Inc., Corning, NY, USA) before the addition of the suspension. Moreover, the lower chamber was filled with RPMI-1640 medium (600 μL) containing 20% FBS. Following 48 hours of incubation at 37 °C, non-attached cells were removed, and invasive cells that adhered to the Matrigel and migratory cells that had entered the lower chamber were fixed in 4% paraformaldehyde for 10 minutes and stained with 0.1% crystal violet (A5104, TCIchemicals, Shanghai, China) for 15 minutes. The number of migratory and invasive cells was determined in eight randomly selected fields using an inverted microscope (TS100, NIKON, Tokyo, Japan) at ×250 magnification.

Murine Xenograft Assay

The experimental protocol involving animals was approved by the Committee of Experimental Animals of Zhejiang Baiyue Biotech Co., Ltd. (approval number: ZJBYLA-IACUC-20211109) and adhered to the guidelines of the Care and Use of Animals in Research and Teaching. Male BALB/c nude mice (n = 18), aged 4–5 weeks, were procured from Beijing HFK Bioscience (Beijing, China). They were housed under controlled conditions of 22–24 °C temperature, 50% humidity, 12/12 h circadian cycle, free access to water, and a standard rat chow.

The mice were divided into three groups using the random number table method, with each group comprising six mice. They were injected subcutaneously with 1×10^6 NCI-H1650 cells transfected with *CLIC5* overexpression plasmids/NC or *CLIC5* and *FTO* overexpression plasmids. Tumor growth was observed every five days using a caliper, and tumor volume was assessed using the formula: (longest diameter) × (shortest diameter)^2 × 0.5.

On the 25th day after the last volume measurement, all the mice were euthanized through spinal dislocation under anesthesia with 3% pentobarbital sodium (50 mg/kg, P010, Sigma-Aldrich, St. Louis, MO, USA). Subsequently, tumors were then harvested, weighed, and underwent qRT-PCR analysis.

qRT-PCR

Total RNA from LC cells, 16HBE cells, and murine tumors was extracted using Trizol reagent (15596018CN, Invitrogen, Carlsbad, CA, USA) and subsequently converted into complementary DNA (cDNA) utilizing SuperScript III First-Strand reverse system (18090010, ThermoFisher, Waltham, MA, USA). qRT-PCR was performed using TB Green Premix Ex Taq (RR420Q, TaKaRa, Tokyo, Japan) on a real-time system (MX3005P, Agilent Technologies, Santa Clara, CA, USA). The primer sequences used in amplification were as follows: *CLIC5*, forward 5′-CTGTGCAGCTGACAGTGAGA-3′ and reverse 5′-GATGGGGCAAAATGGCTGTG-3′; *FTO*, forward 5′-ACTTGGCTCCCTTATCTGACC-3′ and reverse 5′-TGTGCAGTGTGAGAAAGGCTT-3′; glyceraldehyde 3-phosphate dehydrogenase (GAPDH), forward

Journal of
BIOLOGICAL REGULATORS
and Homeostatic Agents

5′-GAGAAGGCTGGGGCTCATTT-3′ and reverse 5′-AGTGATGGCATGGACTGTGG-3′. The amplification conditions were set initial denaturation of 95 °C for 10 minutes, followed by 40 circles of 95 °C for 15 seconds and 60 °C for 1 minute. Relative expression levels of the target genes were assessed using the $2^{-\Delta\Delta Ct}$ method [21] and normalized against GAPDH.

Western Blot

HCC827 cells, NCI-H1650 cells, and murine tumors were lysed using RIPA lysis buffer to obtain total protein. Following quantification utilizing a BCA kit (A53227, ThermoFisher, Waltham, MA, USA), 30 µg of the protein was resolved through 12% SDS-PAGE (P0672, Beyotime, Shanghai, China), and then transferred onto polyvinylidene fluoride membranes (P2438, Sigma-Aldrich, St. Louis, MO, USA) and blocked in Tris Buffered Saline with 1% Tween 20 (TBST, TA-125-TT, ThermoFisher, Waltham, MA, USA) containing 5% non-fat milk for 2 hours at room temperature. After this, the membranes were incubated overnight with primary antibodies against SRC (orb324597, 46 kDa, 1.0 mg/mL, Biorbyt, Cambridge, UK) and GAPDH (orb38656, 36 kDa, 1:1000, Biorbyt, Cambridge, UK) at 4 °C. The next day, after washing with TBST, the membranes underwent a 2-hour incubation with goat anti-rabbit IgG (31460, 1:10,000, ThermoFisher, Waltham, MA, USA) secondary antibody at room temperature. Protein bands were visualized using ECL reagent kits (ab133409, Abcam, Cambridge, UK) coupled with an imager (Tanon-2500, Tanon, Shanghai, China), and densitometry of protein blots was performed using ImageJ software (1.52s version, National Institutes of Health, Bethesda, MA, USA).

Statistical Analysis

Statistical analyses were conducted using GraphPad Prism (version 8.0, GraphPad Software Inc., San Diego, CA, USA). Each experiment was independently repeated three times and the data were expressed as mean ± standard deviation (SD). Differences between the two groups in Fig. 1D–G and Fig. 2 were analyzed using independent *t*-tests. Furthermore, differences among multiple groups were assessed using one-way analysis of variance (ANOVA) and Tukey's post hoc test. A p value of less than 0.05 was considered statistically significant.

Results

Overexpression of CLIC5 Inhibited the Viability, Proliferation, Migration, and Invasion of LC Cells

Utilizing the GEO2R and GSE176348 datasets, *CLIC5* was identified as one of the m^{6}A modification-mediated genes that were differentially expressed in LC. As shown in Fig. 1A, *CLIC5* expression was significantly reduced in LC cells (HCC827, NCI-H23, NCI-H1650, and A549) compared to 16HBE cells ($p < 0.001$). To investigate the role of *CLIC5* in LC, *CLIC5* expression was manipulated by transfecting *CLIC5* overexpression plasmids into HCC827 and NCI-H1650 cells, which originally showed a relatively lower *CLIC5* level compared to other tested cells. Subsequent analysis indicated significant overexpression of *CLIC5* in both HCC827 and NCI-H1650 cells, confirming the successful transfection ($p < 0.001$, Fig. 1B,C). Furthermore, CCK-8 and EdU assays demonstrated that the viability of HCC827 and NCI-H1650 cells overexpressing *CLIC5* was reduced compared to cells transfected with NC at 24 and 48 hours ($p < 0.01$, Fig. 1D,E). Moreover, the number of EdU-positive cells was decreased in HCC827 and NCI-H1650 cells after *CLIC5* overexpression (Fig. 1F–I). Additionally, the Transwell assay revealed that *CLIC5* overexpression attenuated the migratory ($p < 0.01$, Fig. 2A,B) and invasive ($p < 0.01$, Fig. 2C,D) capabilities of HCC827 and NCI-H1650 cells.

FTO Reduced m^{6}A Methylation Levels in LC Cells by Modulating CLIC5 Expression Levels

FTO is a demethylase responsible for alleviating the levels of m^{6}A in LC [6]. We observed reduced m^{6}A levels and elevated *FTO* expression levels in LC cells (HCC827, NCI-H23, NCI-H1650, and A549) compared to 16HBE cells ($p < 0.001$, Fig. 3A,B). Using RMBase v2.0, we obtained sequences related to m^{6}A modification in *CLIC5* and found that *FTO* could bind to one of these sequences (Fig. 3C).

Furthermore, we examined the effect of *FTO* on LC progression regulated by *CLIC5* overexpression. Transfection of sh*FTO*#1/#2 into HCC827 and NCI-H1650 cells resulted in decreased *FTO* levels. Notably, sh*FTO*#1 exhibited a more significant effect ($p < 0.001$, Fig. 3D,E) and was selected for subsequent experiments. MeRIP assay indicated that the m^{6}A methylation of *CLIC5* was potentiated following *FTO* knockdown ($p < 0.001$, Fig. 3F,G).

FTO Overexpression Counteracted the Inhibitory Effect of CLIC5 Overexpression on the Proliferation, Migration, and Invasion of LC Cells

In HCC827 and NCI-H1650 cells, *CLIC5* overexpression had no significant effect on the *FTO* expression (Fig. 4A,C). In contrast, *FTO* overexpression substantially upregulated *FTO* expression levels in HCC827 and NCI-H1650 cells ($p < 0.001$, Fig. 4A,C). Elevated *CLIC5* expression induced by *CLIC5* overexpression plasmids in HCC827 and NCI-H1650 cells was abrogated by *FTO* overexpression ($p < 0.001$, Fig. 4B,D).

Functional assays revealed that *FTO* overexpression reversed the inhibitory effect of *CLIC5* overexpression on the proliferation (Fig. 4E–H), migration ($p < 0.05$, Fig. 5A–C), and invasion ($p < 0.05$, Fig. 5D–F) of HCC827 and NCI-H1650 cells.

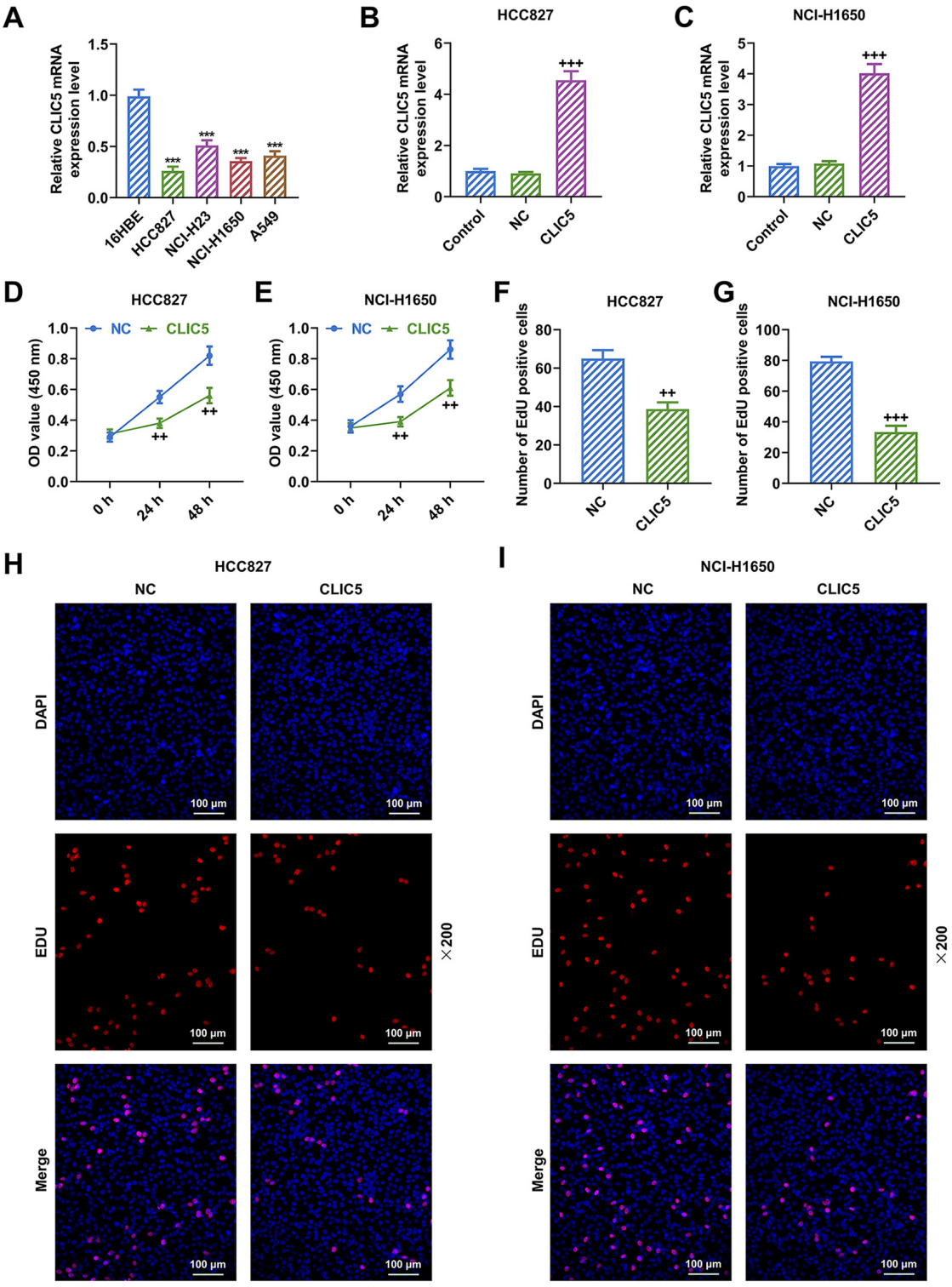

Fig. 1. Overexpression of *CLIC5* inhibited the viability and proliferation of LC cells. (A–C) The expression of *CLIC5* in human LC cells (NCI-H23, NCI-H1650, HCC827, and A549) and 16HBE cells (A), and in HCC827 and NCI-H1650 cells transfected with *CLIC5* overexpression plasmids/NC (B,C) was analyzed by qRT-PCR. GAPDH was used as the internal control. (D,E) The viability of HCC827 and NCI-H1650 cells transfected with *CLIC5* overexpression plasmids or NC was assessed using cell counting kit-8 assay. (F–I) The proliferation of HCC827 and NCI-H1650 cells transfected with *CLIC5* overexpression plasmids/NC was determined utilizing 5-Ethynyl-2′-deoxyuridine (EdU) assay (magnification: ×200; scale: 100 μm). n = 3, $^{***}p < 0.001$ vs 16HBE; $^{++}p < 0.01$, $^{+++}p < 0.001$ vs NC. *CLIC5*, chloride intracellular ion channel 5; qRT-PCR, quantitative reverse transcription polymerase chain reaction; GAPDH, glyceraldehyde 3-phosphate dehydrogenase; NC, negative control; OD, optical density; DAPI, 4′,6-diamidino-2-phenylindole.

Journal of
BIOLOGICAL REGULATORS
and Homeostatic Agents

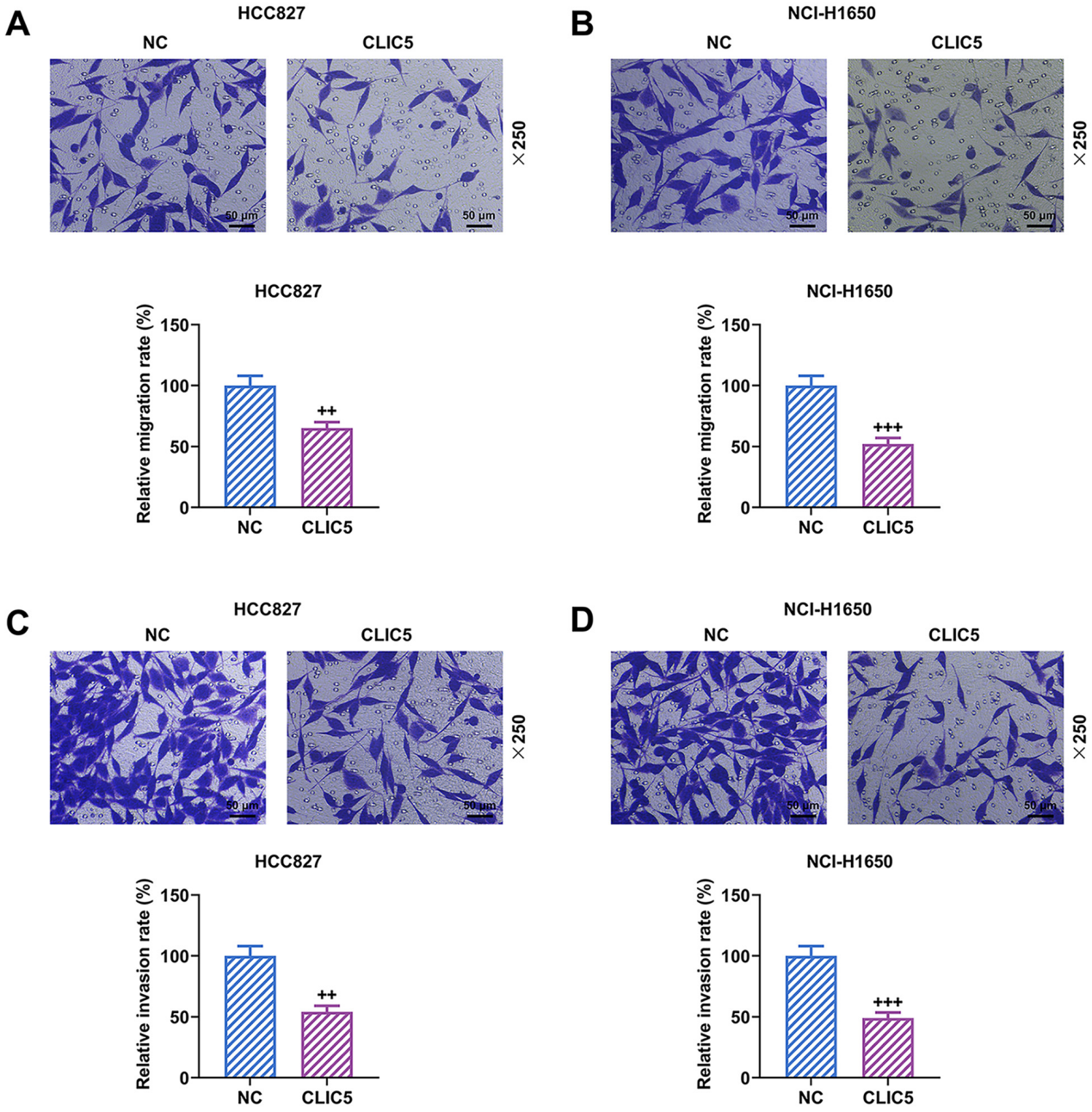

Fig. 2. *CLIC5* overexpression inhibited LC cell migration and invasion. (A–D) The migratory (A,B) and invasive (C,D) capabilities of HCC827 and NCI-H1650 cells transfected with *CLIC5* overexpression plasmids/NC were assessed using Transwell assay (magnification: ×250; scale: 50 μm). n = 3, $^{++}p < 0.01$, $^{+++}p < 0.001$ vs NC. *CLIC5*, chloride intracellular ion channel 5; NC, negative control.

FTO Overexpression Reversed the Suppressing Effect of CLIC5 Overexpression on Lung Tumorigenesis in Vivo

A murine xenograft assay was conducted to ascertain the role of *FTO* and *CLIC5* in lung tumorigenesis *in vivo*. As illustrated in Fig. 6A–C, *CLIC5* overexpression inhibited tumor growth and diminished tumor volume and weight ($p < 0.01$). Notably, *FTO* overexpression significantly reversed the effect of *CLIC5* overexpression by increasing tumor volume and weight ($p < 0.05$). Furthermore, within the tumors, *CLIC5* overexpression substantially increased *CLIC5* levels ($p < 0.01$, Fig. 6E) while only slightly impacting *FTO* levels (Fig. 6D). Conversely, overexpression of *FTO* significantly upregulated *FTO* levels in *CLIC5*-overexpressing tumors ($p < 0.001$, Fig. 6D) and reversed the effect of *CLIC5* overexpression on *CLIC5* levels within the tumors ($p < 0.001$, Fig. 6E).

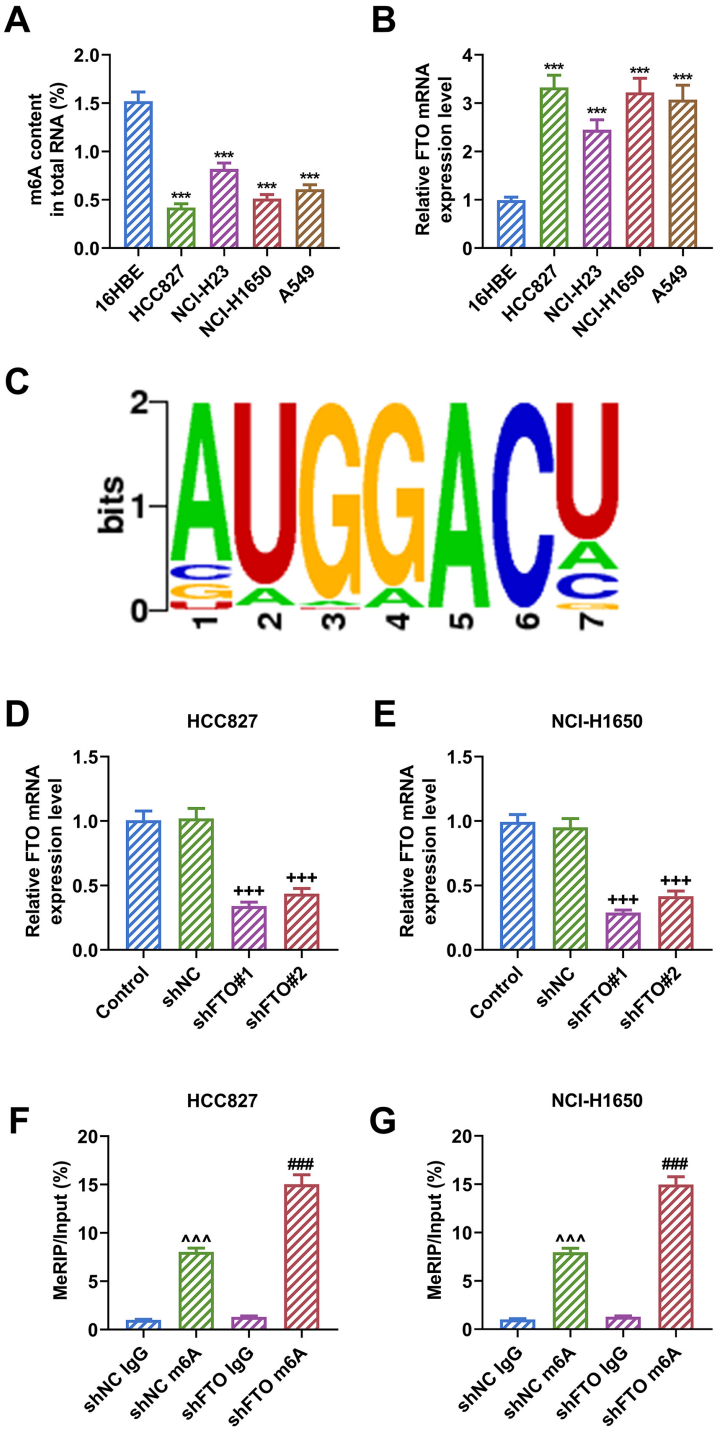

Fig. 3. *FTO* reduced m^{6}A methylation levels in LC cells by modulating *CLIC5* expression levels. (A) The overall m^{6}A levels in human LC cells (NCI-H23, NCI-H1650, HCC827, and A549) and 16HBE cells were determined using assay kits. (B) The expression of *FTO* in human LC and 16HBE cells was analyzed using qRT-PCR, with GAPDH as the internal control. (C) The sequence alignment between *FTO* and the sites for m^{6}A in *CLIC5* was identified using RMBase v2.0. (D,E) The expression of *FTO* in HCC827 and NCI-H1650 cells transfected with sh*FTO*#1/#2/shNC was quantified utilizing qRT-PCR, with GAPDH as the internal control. (F,G) The interaction between *FTO* and the m^{6}A modification of *CLIC5* within HCC827 and NCI-H1650 cells transfected with sh*FTO*/shNC was determined employing a methylated RNA immunoprecipitation assay. n = 3, $^{***}p < 0.001$ vs 16HBE; $^{+++}p < 0.001$ vs shNC; $^{\wedge\wedge\wedge}p < 0.001$ vs shNC lgG; $^{\#\#\#}p < 0.001$ vs sh*FTO* lgG. m^{6}A, N6-methyladenosine; *CLIC5*, chloride intracellular ion channel 5; *FTO*, fat mass and obesity-associated protein; qRT-PCR, quantitative reverse transcription polymerase chain reaction; GAPDH, glyceraldehyde 3-phosphate dehydrogenase; NC, negative control; sh*FTO*, short hairpin RNA against *FTO*; shNC, short hairpin RNA against NC.

Journal of
BIOLOGICAL REGULATORS
and Homeostatic Agents

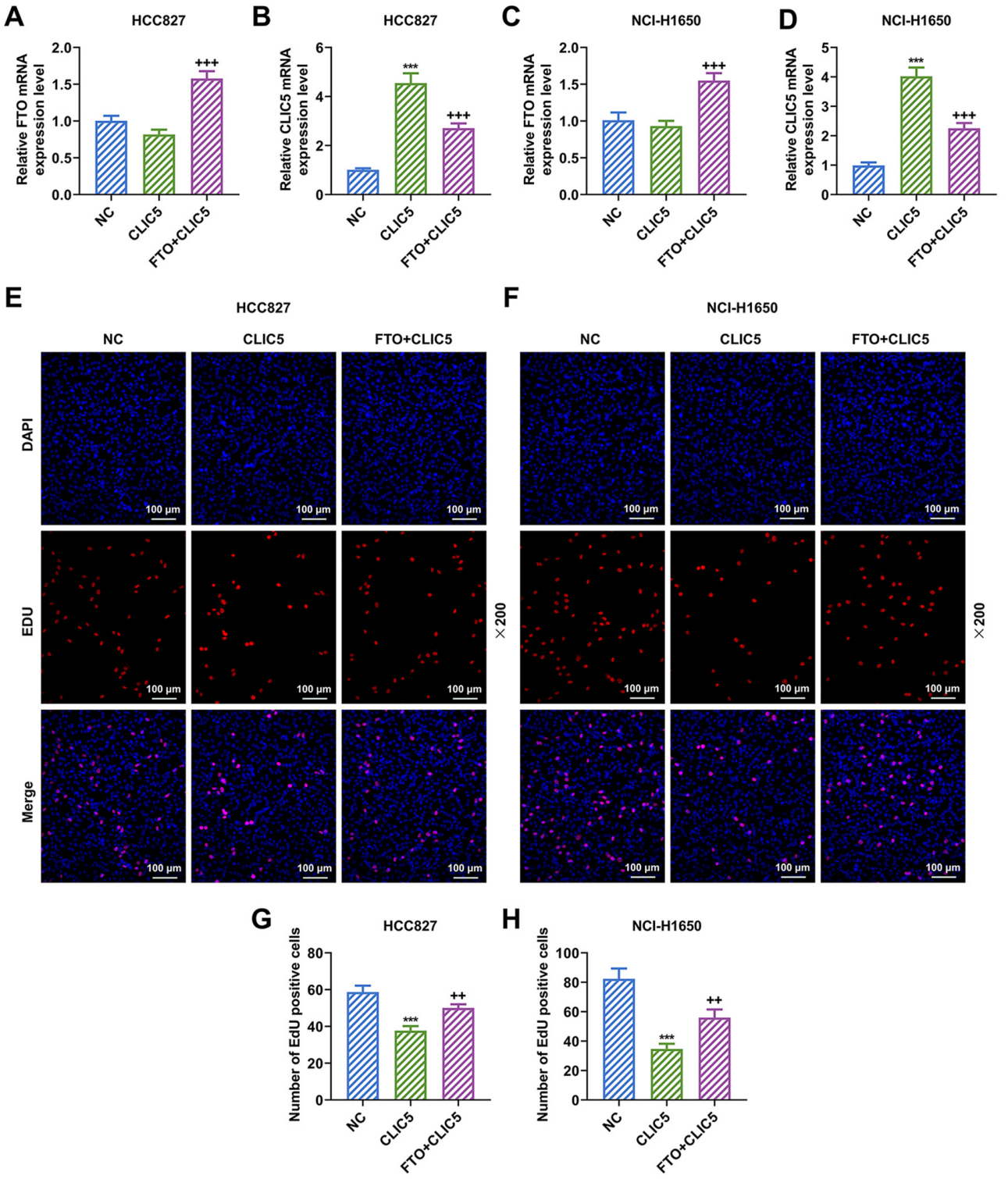

Fig. 4. *FTO* overexpression counteracted the effect of *CLIC5* overexpression on LC cell proliferation. (A–D) The expression levels of *FTO* (A,C) and *CLIC5* (B,D) in HCC827 and NCI-H1650 cells transfected with *CLIC5* overexpression plasmids/NC or *CLIC5* and *FTO* overexpression plasmids were analyzed using qRT-PCR, with GAPDH as the internal control. (E–H) The proliferation of HCC827 and NCI-H1650 cells transfected with *CLIC5* overexpression plasmids/NC or *CLIC5* and *FTO* overexpression plasmids was determined utilizing EdU assay (magnification: ×200; scale: 100 μm). n = 3, ***$p < 0.001$ vs NC; $^{++}p < 0.01$, $^{+++}p < 0.001$ vs *CLIC5*. *CLIC5*, chloride intracellular ion channel 5; *FTO*, fat mass and obesity-associated protein; qRT-PCR, quantitative reverse transcription polymerase chain reaction; GAPDH, glyceraldehyde 3-phosphate dehydrogenase; NC, negative control.

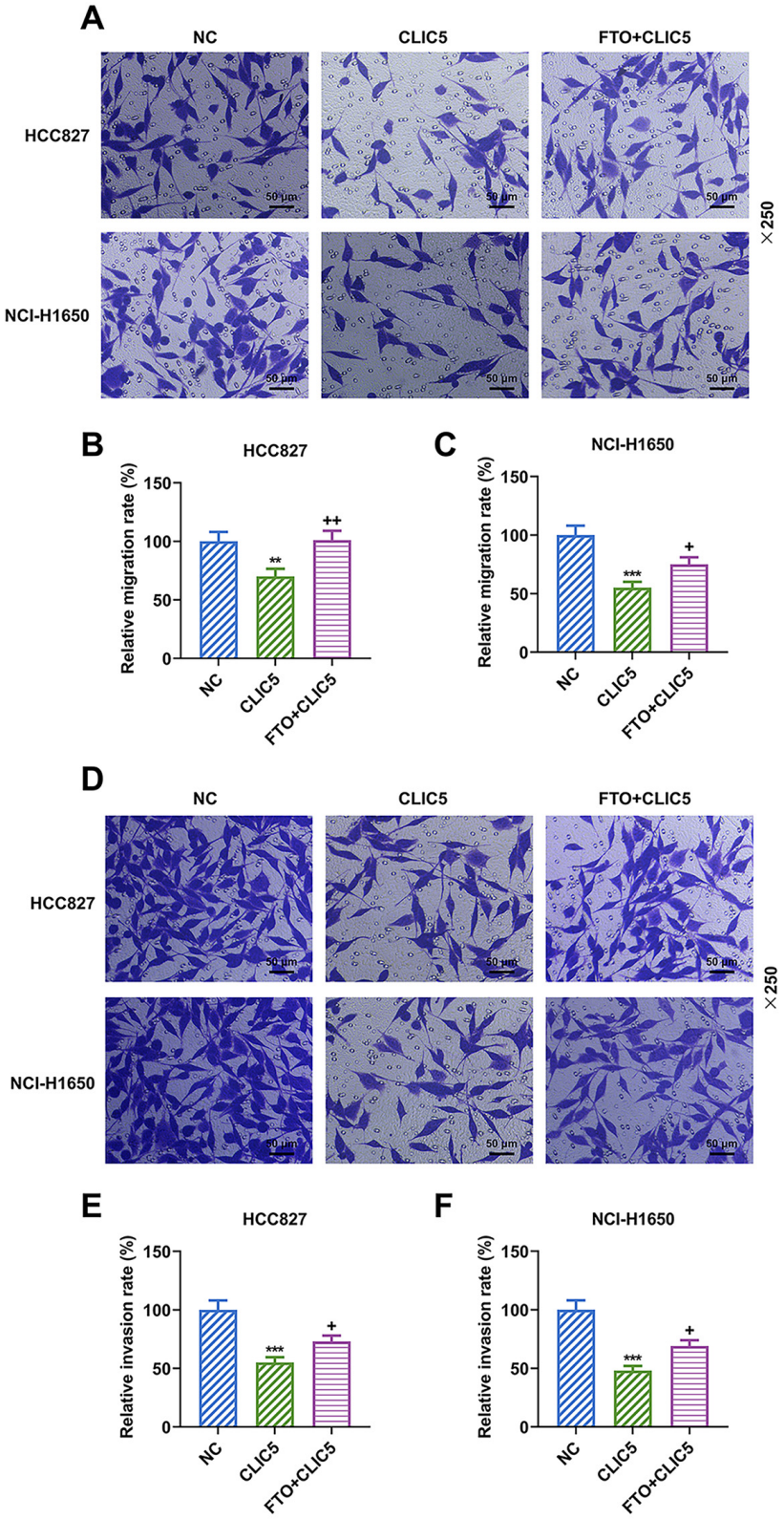

Fig. 5. *FTO* overexpression counteracted the effect of *CLIC5* overexpression on the LC cell migration and invasion. (A–F) The migratory (A–C) and invasive (D–F) capabilities of HCC827 and NCI-H1650 cells transfected with *CLIC5* overexpression plasmids/NC or *CLIC5* and *FTO* overexpression plasmids were assessed employing Transwell assay (magnification: ×250; scale: 50 μm). n = 3, $^{**}p < 0.01$,$^{***}p < 0.001$ vs NC; $^{+}p < 0.05$, $^{++}p < 0.01$ vs *CLIC5*. *CLIC5*, chloride intracellular ion channel 5; *FTO*, fat mass and obesity-associated protein; NC, negative control.

Journal of
BIOLOGICAL REGULATORS
and Homeostatic Agents

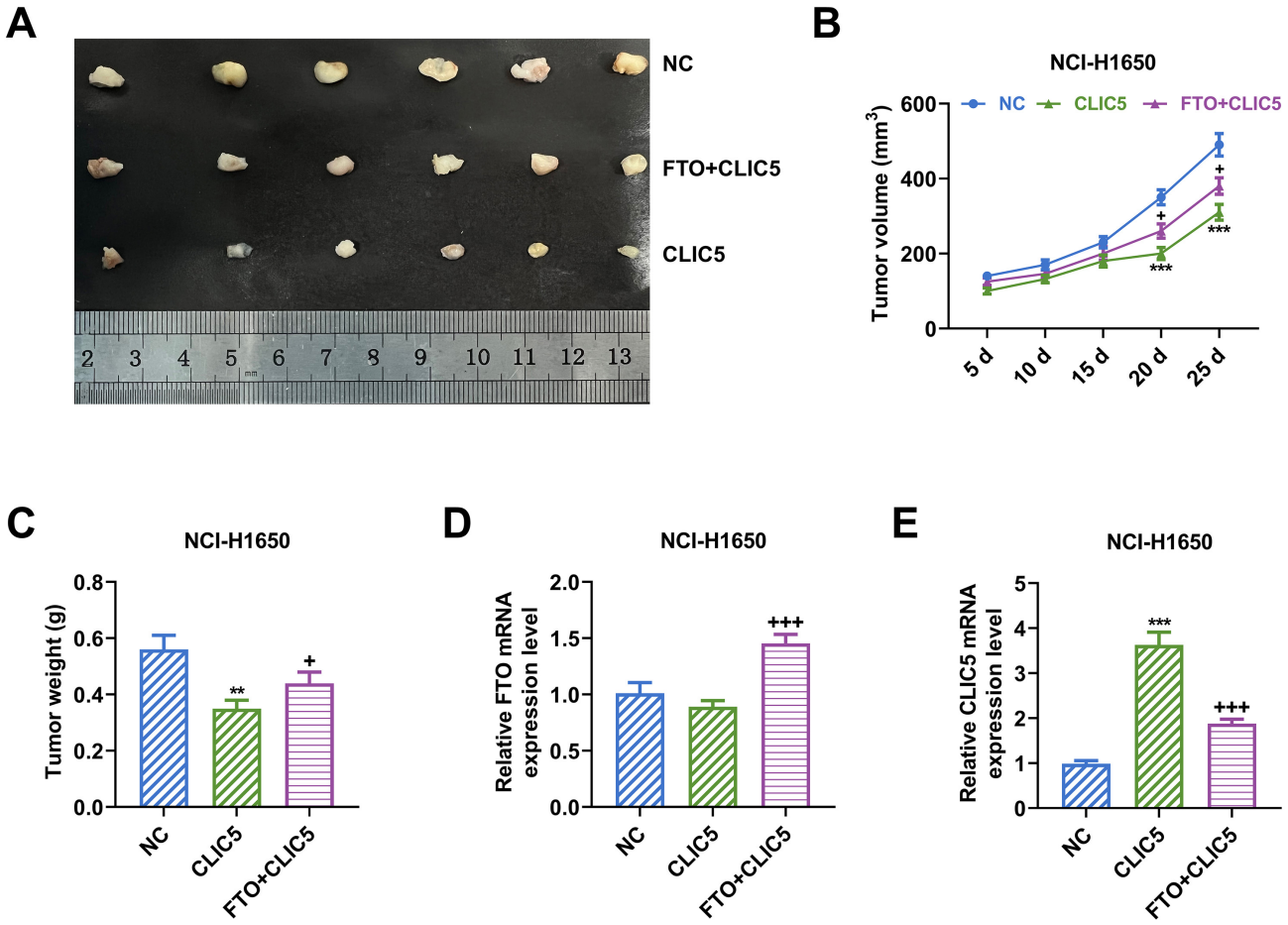

Fig. 6. *FTO* overexpression reversed the effect of *CLIC5* overexpression on lung tumorigenesis *in vivo*. (A–E) The tumorigenic ability of NCI-H1650 cells transfected with *CLIC5* overexpression plasmids/NC or *CLIC5* and *FTO* overexpression plasmids was evaluated using murine xenograft assay. Tumor volume was monitored every five days (A,B), and the tumor weight was assessed at the end of the experiment (C), n = 6. Within the tumors, the expressions of *FTO* and *CLIC5* were analyzed using qRT-PCR (D,E), with GAPDH as the internal control. n = 3, ** $p < 0.01$, *** $p < 0.001$ vs NC; $^{+}p < 0.05$, $^{+++}p < 0.001$ vs *CLIC5*. *CLIC5*, chloride intracellular ion channel 5; *FTO*, fat mass and obesity-associated protein; qRT-PCR, quantitative reverse transcription polymerase chain reaction; GAPDH, glyceraldehyde 3-phosphate dehydrogenase; NC, negative control.

SRC Could Interact with CLIC5 and was Regulated by the FTO/CLIC5 Axis in LC

The downstream mechanism of *CLIC5* was explored using STRING, which predicted an interaction between *CLIC5* and SRC (Fig. 7A). A previous study has demonstrated elevated expression levels of SRC in LC [22]. Consistently, our analyses based on starBase indicated significantly higher SRC expression in LC samples compared to normal samples ($p = 5.7 \times 10^{-10}$, Fig. 7B). Moreover, SRC expression was repressed in HCC827 and NCI-H1650 cells, as well as in NCI-H1650 cell-induced tumors after *CLIC5* overexpression ($p < 0.01$, Fig. 7C–E), which was counteracted by *FTO* overexpression ($p < 0.05$, Fig. 7C–E).

Discussion

Currently, identifying an increasing number of clinically significant genetic variants through molecular testing, utilizing minimally invasive techniques with relatively small sample sizes, remains a considerable challenge [23]. Therefore, it is crucial to prioritize an understanding of the molecular mechanism underlying LC pathogenesis and progression.

Genome-wide meta-analyses have revealed that aberrantly expressed CLICs are localized in several types of cancer tissues [24–26], suggesting their role in cancer progression. Specifically, *CLIC5*, a member of the CLICs family, is predominantly located in the inner mitochondrial membrane, where it is thought to modulate reactive oxygen species, thereby affecting tumor signaling [14]. A meta-analysis based on comprehensive and updated data

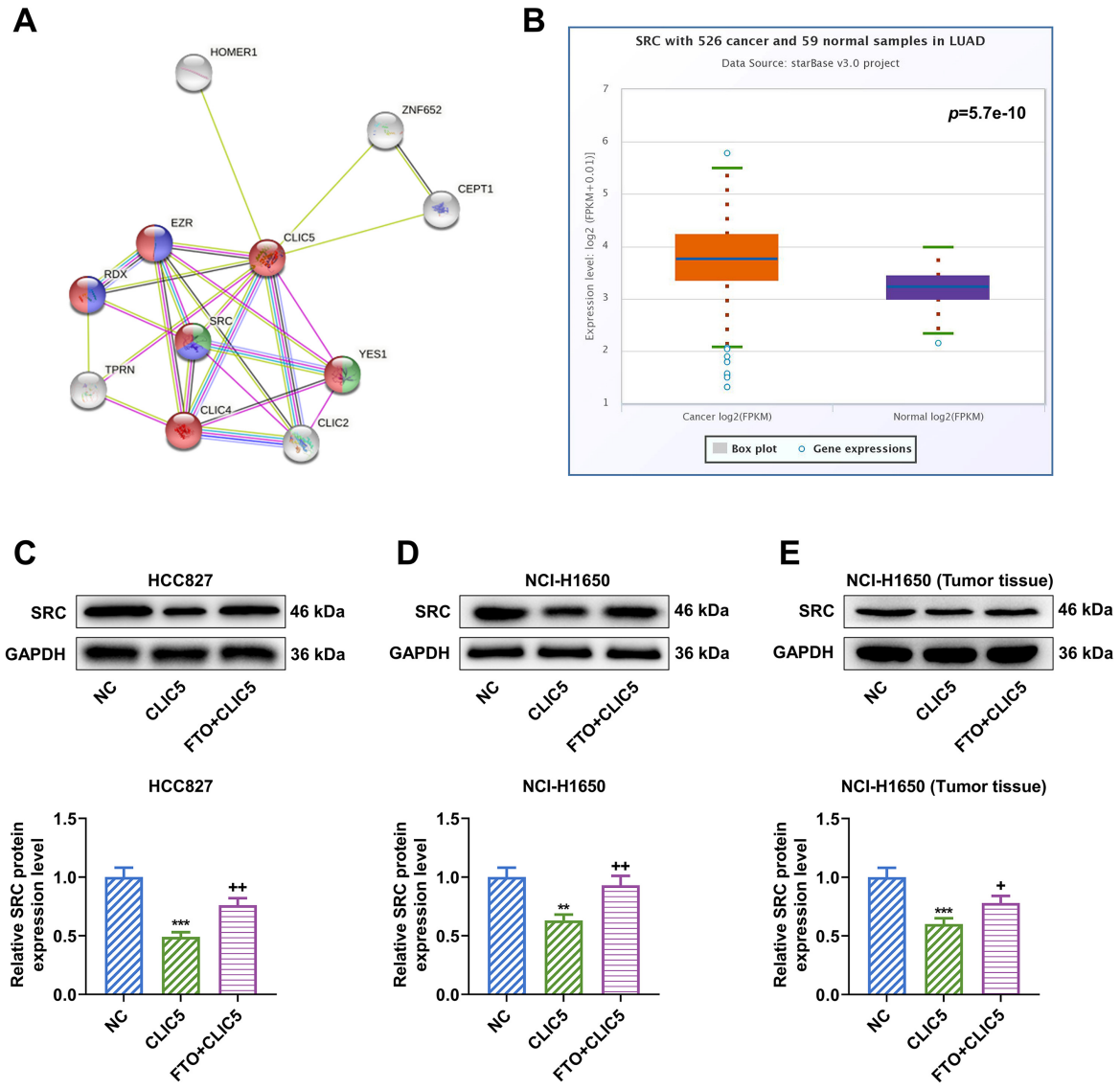

Fig. 7. SRC could interact with CLIC5 and was regulated by the *FTO*/*CLIC5* axis in LC. (A,B) The interaction between CLIC5 and SRC was predicted using STRING (A), and the expression of SRC in LC was analyzed through StarBase (B). (C–E) The expression of SRC in HCC827 and NCI-H1650 cells transfected with CLIC5 overexpression plasmids/NC or CLIC5 and FTO overexpression plasmids (C,D) and in murine tumors (E) was analyzed utilizing Western blot analysis, with GAPDH as the internal control. n = 3, ** $p < 0.01$, *** $p < 0.001$ vs NC; $^{+}p < 0.05$, $^{++}p < 0.01$ vs *CLIC5*. CLIC5, chloride intracellular ion channel 5; FTO, fat mass and obesity-associated protein; NC, negative control; SRC, proto-oncogene tyrosine-protein kinase SRC.

has revealed that high *CLIC5* expression is associated with shorter survival time in ovarian cancer and pancreatic cancer but with longer survival time in breast cancer, gastric cancer, liver cancer, and LC [14]. These findings imply that *CLIC5* expression may either promote or suppress the progression of certain cancer, with elevated *CLIC5* expression repressing LC progression. Previous studies have shown that elevated *CLIC5* expression in ALL induces leukemogenesis [15], whereas reduced *CLIC5* expression in HCC results in decreased cell migration and invasion [16]. Moreover, the upregulation of *CLIC5* in PDAC is correlated with cell growth and invasion [27]. On the contrary, *CLIC5* expression is reduced in osteosarcoma [18], a pattern similar to our findings based on qRT-PCR analysis in cells. Furthermore, our functional assay showed that *CLIC5* overexpression dampened LC cell viability, migration, and invasion while suppressing lung tumor growth, manifesting that *CLIC5* acts as a tumor suppressor in LC.

m^6A methylation is an active research area in epigenetic modification pertinent to LC progression [6]. LC tissues exhibit reduced overall m^6A levels [6], consistent with our findings in LC cells. *CLIC5* has been proven to undergo differential methylation in neuroblastoma [28]. *FTO*, identified as the first m^6A eraser, exerts an oxida-

Journal of
BIOLOGICAL REGULATORS
and Homeostatic Agents

tive function that effectively demethylates m^6A in RNA [8]. *FTO* plays a role in controlling feeding behavior and energy expenditure and has been associated with human obesity [8,29]. *FTO* is implicated in carcinogenesis, playing different regulatory roles [30]. In acute myeloid leukemia (AML) [31,32] and melanoma [33], overexpression of *FTO* reduces m^6A methylation in target mRNA transcript, exerting oncogenic effects. Therapeutic strategies targeting *FTO* have achieved massive cytotoxicity against leukemia and glioma cells [34].

In our study, *FTO* was expressed abundantly opposite to m^6A in LC cells, as shown in previous research [6]. RMBase v2.0-based prediction and MeRIP assay unveiled that *FTO* could bind to one of the m^6A sites on *CLIC5,* abrogating the transfection-mediated overexpression of *CLIC5* in LC cells. These results, combined with previous research attributing decreased overall m^6A level in LC to increased level of *FTO* [6], suggest that *FTO* demethylates the m^6A modification of *CLIC5,* resulting in its downregulation in LC. Moreover, our study demonstrated that overexpression of *FTO* counteracted the suppressive effect of *CLIC5* overexpression on LC cell proliferation, migration, and invasion, and *in vivo* tumorigenesis, which indicates that *FTO*-mediated m^6A demethylation downregulates *CLIC5,* thereby promoting LC progression.

Additionally, in our study, the PPI prediction using STRING illustrated that *CLIC5* can interact with SRC, which is highly expressed in LC [22]. SRC is a cellular tyrosine kinase critically implicated in tumorigenic and metastatic processes [35,36]. Evidence has shown that SRC activates STAT3 signaling and focal adhesion kinase signaling, strongly correlated with tumorigenesis [37], facilitating tumor-sphere formation, enhancing stemness, and promoting the migration and invasion of LC cells [22,38]. Targeting SRC offers a potential therapeutic strategy for LC [35]. Through StarBase-based prediction, SRC was reaffirmed to be expressed highly in LC. Moreover, we observed that in LC cells, overexpressing *CLIC5* repressed SRC expression, which was reversed by *FTO* overexpression. These results, combined with the findings mentioned above regarding SRC, indicate that SRC upregulation may serve as the downstream mechanism of *FTO*-mediated m^6A demethylation of *CLIC5*, contributing to the promotion of LC progression.

There are some limitations to this study, in order to better elucidate the functional relationship between FTO and CLIC5, we should set FTO overexpression or knockdown group for experimental analysis. In addition, the expression of FTO and CLIC5 in patients with different stages or subtypes of Lung cancer and their relationship with prognosis were not analyzed. In the future, it will be necessary to collect clinical samples to evaluate the clinical significance and potential therapeutic value of FTO and CLIC5.

Conclusions

In conclusion, our study demonstrates that *CLIC5* is downregulated in LC, and its overexpression inhibits LC progression *in vitro* and *in vivo*. Furthermore, we unveil that *FTO*-mediated m^6A demethylation of *CLIC5* is responsible for low expression of *CLIC5* in LC, leading to the upregulation of SRC. These findings provide novel insights into LC progression through an m^6A demethylation-related mechanism.

Availability of Data and Materials

The analyzed data sets generated during the study are available from the corresponding author on reasonable request.

Author Contributions

Substantial contributions to conception and design: YX. Data acquisition, data analysis and interpretation: ZL, ZC, LH, HW. Drafting this manuscript: all authors. Contributing to important editorial changes for intellectual content: all authors. Final approval of the version to be published: all authors. Agreement to be accountable for all aspects of the work in ensuring that questions related to the accuracy or integrity of the work are appropriately investigated and resolved: all authors.

Ethics Approval and Consent to Participate

All animal experiments were performed according to the procedure approved by the Committee of Experimental Animals of Zhejiang Baiyue Biotech Co., Ltd. (approval number: ZJBYLA-IACUC-20211109) and followed the guidelines of the Care and Use of Animals in Research and Teaching.

Acknowledgment

Not applicable.

Funding

This work was supported by the Medical Research Fund Project of Guangdong Province (B2021364).

Conflict of Interest

The authors declare no conflict of interest.

References

[1] Li H, Zhang Y, Guo Y, Liu R, Yu Q, Gong L, *et al*. ALKBH1 promotes lung cancer by regulating m6A RNA demethylation. Biochemical Pharmacology. 2021; 189: 114284.
[2] Siegel RL, Miller KD, Jemal A. Cancer statistics, 2018. CA: a Cancer Journal for Clinicians. 2018; 68: 7–30.
[3] Didkowska J, Wojciechowska U, Mańczuk M, Łobaszewski J. Lung cancer epidemiology: contemporary and future challenges worldwide. Annals of Translational Medicine. 2016; 4: 150.

[4] de Sousa VML, Carvalho L. Heterogeneity in Lung Cancer. Pathobiology: Journal of Immunopathology, Molecular and Cellular Biology. 2018; 85: 96–107.
[5] Li Y, Gu J, Xu F, Zhu Q, Chen Y, Ge D, *et al*. Molecular characterization, biological function, tumor microenvironment association and clinical significance of m6A regulators in lung adenocarcinoma. Briefings in Bioinformatics. 2021; 22: bbaa225.
[6] Sun J, Ping Y, Huang J, Zeng B, Ji P, Li D. N6-Methyladenosine-Regulated mRNAs: Potential Prognostic Biomarkers for Patients With Lung Adenocarcinoma. Frontiers in Cell and Developmental Biology. 2021; 9: 705962.
[7] Bauer M, Vaxevanis C, Heimer N, Al-Ali HK, Jaekel N, Bachmann M, *et al*. Expression, Regulation and Function of microRNA as Important Players in the Transition of MDS to Secondary AML and Their Cross Talk to RNA-Binding Proteins. International Journal of Molecular Sciences. 2020; 21: 7140.
[8] Jia G, Fu Y, Zhao X, Dai Q, Zheng G, Yang Y, *et al*. N6-methyladenosine in nuclear RNA is a major substrate of the obesity-associated *FTO*. Nature Chemical Biology. 2011; 7: 885–887.
[9] Niu Y, Lin Z, Wan A, Chen H, Liang H, Sun L, *et al*. RNA N6-methyladenosine demethylase *FTO* promotes breast tumor progression through inhibiting BNIP3. Molecular Cancer. 2019; 18: 46.
[10] Tao L, Mu X, Chen H, Jin D, Zhang R, Zhao Y, *et al*. *FTO* modifies the m6A level of MALAT and promotes bladder cancer progression. Clinical and Translational Medicine. 2021; 11: e310.
[11] Li J, Han Y, Zhang H, Qian Z, Jia W, Gao Y, *et al*. The m6A demethylase *FTO* promotes the growth of lung cancer cells by regulating the m6A level of USP7 mRNA. Biochemical and Biophysical Research Communications. 2019; 512: 479–485.
[12] Ponnalagu D, Singh H. Anion Channels of Mitochondria. Handbook of Experimental Pharmacology. 2017; 240: 71–101.
[13] Suh KS, Yuspa SH. Intracellular chloride channels: critical mediators of cell viability and potential targets for cancer therapy. Current Pharmaceutical Design. 2005; 11: 2753–2764.
[14] Gururaja Rao S, Patel NJ, Singh H. Intracellular Chloride Channels: Novel Biomarkers in Diseases. Frontiers in Physiology. 2020; 11: 96.
[15] Neveu B, Spinella JF, Richer C, Lagacé K, Cassart P, Lajoie M, *et al*. CLIC5: a novel ETV6 target gene in childhood acute lymphoblastic leukemia. Haematologica. 2016; 101: 1534–1543.
[16] Flores-Téllez TNJ, Lopez TV, Vásquez Garzón VR, Villa-Treviño S. Co-Expression of Ezrin-CLIC5-Podocalyxin Is Associated with Migration and Invasiveness in Hepatocellular Carcinoma. PloS One. 2015; 10: e0131605.
[17] Magouliotis DE, Sakellaridis N, Dimas K, Tasiopoulou VS, Svokos KA, Svokos AA, *et al*. *In Silico* Transcriptomic Analysis of the Chloride Intracellular Channels (CLIC) Interactome Identifies a Molecular Panel of Seven Prognostic Markers in Patients with Pancreatic Ductal Adenocarcinoma. Current Genomics. 2020; 21: 119–127.
[18] Liu J, Wu S, Xie X, Wang Z, Lei Q. The role of significantly deregulated MicroRNAs in osteosarcoma based on bioinformatic analysis. Technology and Health Care: Official Journal of the European Society for Engineering and Medicine. 2021; 29: 333–341.
[19] He Q, Dong Y, Zhu Y, Ding Z, Zhang X, Wang Z, *et al*. TMEM100 induces cell death in non small cell lung cancer via the activation of autophagy and apoptosis. Oncology Reports. 2021; 45: 63.
[20] Legendre M, Butt A, Borie R, Debray MP, Bouvry D, Filhol-Blin E, *et al*. Functional assessment and phenotypic heterogeneity of *SFTPA1* and *SFTPA2* mutations in interstitial lung diseases and lung cancer. The European Respiratory Journal. 2020; 56: 2002806.
[21] Livak KJ, Schmittgen TD. Analysis of relative gene expression data using real-time quantitative PCR and the 2(-Delta Delta C(T)) Method. Methods (San Diego, Calif.). 2001; 25: 402–408.
[22] Liu W, Liang Y, Chan Q, Jiang L, Dong J. CX3CL1 promotes lung cancer cell migration and invasion via the Src/focal adhesion kinase signaling pathway. Oncology Reports. 2019; 41: 1911–1917.
[23] Hiley CT, Le Quesne J, Santis G, Sharpe R, de Castro DG, Middleton G, *et al*. Challenges in molecular testing in non-small-cell lung cancer patients with advanced disease. Lancet (London, England). 2016; 388: 1002–1011.
[24] Yau C, Esserman L, Moore DH, Waldman F, Sninsky J, Benz CC. A multigene predictor of metastatic outcome in early stage hormone receptor-negative and triple-negative breast cancer. Breast Cancer Research: BCR. 2010; 12: R85.
[25] Supiot S, Gouraud W, Campion L, Jezéquel P, Buecher B, Charrier J, *et al*. Early dynamic transcriptomic changes during preoperative radiotherapy in patients with rectal cancer: a feasibility study. World Journal of Gastroenterology. 2013; 19: 3249–3254.
[26] Ge YZ, Xu Z, Xu LW, Yu P, Zhao Y, Xin H, *et al*. Pathway analysis of genome-wide association study on serum prostate-specific antigen levels. Gene. 2014; 551: 86–91.
[27] Wong CH, Li CH, He Q, Chan SL, Tong JHM, To KF, *et al*. Ectopic HOTTIP expression induces noncanonical transactivation pathways to promote growth and invasiveness in pancreatic ductal adenocarcinoma. Cancer Letters. 2020; 477: 1–9.
[28] Olsson M, Beck S, Kogner P, Martinsson T, Carén H. Genome-wide methylation profiling identifies novel methylated genes in neuroblastoma tumors. Epigenetics. 2016; 11: 74–84.
[29] Fawcett KA, Barroso I. The genetics of obesity: *FTO* leads the way. Trends in Genetics: TIG. 2010; 26: 266–274.
[30] Relier S, Rivals E, David A. The multifaceted functions of the Fat mass and Obesity-associated protein (*FTO*) in normal and cancer cells. RNA Biology. 2022; 19: 132–142.
[31] Su R, Dong L, Li Y, Gao M, Han L, Wunderlich M, *et al*. Targeting *FTO* Suppresses Cancer Stem Cell Maintenance and Immune Evasion. Cancer Cell. 2020; 38: 79–96.e11.
[32] Li Z, Weng H, Su R, Weng X, Zuo Z, Li C, *et al*. *FTO* Plays an Oncogenic Role in Acute Myeloid Leukemia as a N^6-Methyladenosine RNA Demethylase. Cancer Cell. 2017; 31: 127–141.
[33] Yang S, Wei J, Cui YH, Park G, Shah P, Deng Y, *et al*. m^6A mRNA demethylase *FTO* regulates melanoma tumorigenicity and response to anti-PD-1 blockade. Nature Communications. 2019; 10: 2782.
[34] . R-2HG Targets *FTO* to Increase m^6A Levels and Suppress Tumor Growth. Cancer Discovery. 2018; 8: 137.
[35] Giaccone G, Zucali PA. Src as a potential therapeutic target in non-small-cell lung cancer. Annals of Oncology: Official Journal of the European Society for Medical Oncology. 2008; 19: 1219–1223.
[36] Summy JM, Gallick GE. Src family kinases in tumor progression and metastasis. Cancer Metastasis Reviews. 2003; 22: 337–358.
[37] Liu Z, Ma L, Sun Y, Yu W, Wang X. Targeting STAT3 signaling overcomes gefitinib resistance in non-small cell lung cancer. Cell Death & Disease. 2021; 12: 561.
[38] Bhummaphan N, Petpiroon N, Prakhongcheep O, Sritularak B, Chanvorachote P. Lusianthridin targeting of lung cancer stem cells via Src-STAT3 suppression. Phytomedicine: International Journal of Phytotherapy and Phytopharmacology. 2019; 62: 152932.